Increase in HFC-134a emissions in response to the success of the Montreal Protocol

A. Fortems-Cheiney[1,2], M. Saunois[1], I. Pison[1], F. Chevallier[1], P. Bousquet[1], C. Cressot[1], S. A. Montzka[3], P. J. Fraser[4], M. K. Vollmer[5], P. G. Simmonds[6], D. Young[6], S. O'Doherty[6], R. F. Weiss[7], F. Artuso[8], B. Barletta[9], D. R. Blake[9], S. Li[10], C. Lunder[11], B. R. Miller[3], S. Park[10,12], R. Prinn[13], T. Saito[14], L. P. Steele[4], and Y. Yokouchi[14]

[1]Laboratoire des Sciences du Climat et de l'Environnement, Institut Pierre-Simon Laplace, CEA/CNRS/UVSQ, Gif-sur-Yvette, France, [2]Now at Laboratoire Interuniversitaire des Systèmes Atmosphériques, CNRS/INSU UMR7583, Université Paris-Est Créteil et Université Paris Diderot, Institut Pierre-Simon Laplace, Créteil, France, [3]Earth System Research Laboratory, National Oceanic and Atmospheric Administration, Boulder, Colorado, USA, [4]CSIRO Oceans and Atmosphere Flagship, Aspendale, Victoria, Australia, [5]Laboratory for Air Pollution and Environmental Technology, Empa, Swiss Federal Laboratories for Materials Science and Technology, Dubendorf, Switzerland, [6]School of Chemistry, University of Bristol, Bristol, UK, [7]Scripps Institution of Oceanography, University of California, San Diego, La Jolla, California, USA, [8]Italian National Agency for New Technologies, Energy and Sustainable Economic Development, Rome, Italy, [9]Department of Chemistry, University of California, Irvine, California, USA, [10]Kyungpook Institute of Oceanography, College of Natural Sciences, Kyungpook National University, Daegu, South Korea, [11]Norwegian Institute for Air Research, Kjeller, Norway, [12]Department of Oceanography, College of Ecology and Environmental Science, Kyungpook National University, Sangju, South Korea, [13]Center for Global Change Science, Massachusetts Institute of Technology, Cambridge, Massachusetts, USA, [14]National Institute for Environmental Studies, Tsukuba, Japan

Abstract The 1,1,1,2-tetrafluoroethane (HFC-134a), an important alternative to CFC-12 in accordance with the Montreal Protocol on Substances that Deplete the Ozone Layer, is a high global warming potential greenhouse gas. Here we evaluate variations in global and regional HFC-134a emissions and emission trends, from 1995 to 2010, at a relatively high spatial and temporal (3.75° in longitude × 2.5° in latitude and 8 day) resolution, using surface HFC-134a measurements. Our results show a progressive increase of global HFC-134a emissions from 19 ± 2 Gg/yr in 1995 to 167 ± 5 Gg/yr in 2010, with both a slowdown in developed countries and a 20%/yr increase in China since 2005. A seasonal cycle is also seen since 2002, which becomes enhanced over time, with larger values during the boreal summer.

1. Introduction

As a consequence of the Montreal Protocol and its amendments, hydrofluorocarbons (HFCs) have been introduced as replacement compounds for both chlorofluorocarbons (CFCs) and hydrochlorofluorocarbons (HCFCs) since they do not deplete stratospheric ozone. The most abundant HFC measured in the atmosphere is HFC-134a [*Carpenter et al.*, 2014]. HFC-134a has a steady state lifetime of 14 years; it is mainly removed from the atmosphere by its reaction with hydroxyl radicals (OH) and to a lesser extent by oxidation and photolysis in the stratosphere [*Carpenter et al.*, 2014]. Its global average mixing ratio reached about 68 ppt (parts per trillion) in 2012 and has steadily increased, with a growth rate of 5 ppt/yr over the period 2011–2012 [*Carpenter et al.*, 2014], similar to the growth rate of 4.7 ppt/yr over the period 2005–2008 [*Montzka et al.*, 2011].

While posing no threat to stratospheric ozone, HFC-134a is nevertheless of concern because of its long lifetime, combined with a relatively high global warming potential (GWP) of 1500 over the 100 year horizon [*Forster et al.*, 2007; *Harris et al.*, 2014]. Indeed, the HFC-134a contribution to atmospheric radiative forcing has grown from negligible in 1995 to 12 ± 0.2 mW/m^2 in recent years [*Rigby et al.*, 2014] following the sharp emission rise over this period. Within current scenarios of continued HFC emission growth, its contribution to the radiative forcing of the climate system could be equivalent to 9–19% of carbon dioxide emissions by the year 2050 [*Velders et al.*, 2009; *Daniel et al.*, 2011]. Amendment proposals to address HFCs under the Montreal Protocol have been submitted in May 2014 [*Environmental Protection Agency* (*EPA*), 2014]. Since low GWP products exist for replacement of HFC-134a and for use in refrigeration and air-conditioning systems, HFC-134a is a key candidate for climate mitigation and it has come into the focus of international climate policy [*Molina et al.*, 2009]. There is a growing interest in better estimating global and regional emissions of this species.

HFC-134a has been the preferred replacement gas of CFC-12 (CCl_2F_2) in developed countries. According to the Alternative Fluorocarbons Environmental Acceptability Study (www.afeas.org), in 2001, over 80% of the worldwide sales of HFC-134a fall into two categories: mobile air conditioning (MAC) and commercial refrigeration (in order of importance, HFC-134a from MAC reaching 70% of the global emissions [*Montzka et al.*, 2014]). These emission sources are the most important in Europe [*Schwarz and Harnisch*, 2003] and in the U.S. [*EPA*, 2008]. HFC-134a is emitted from air-conditioning systems to the atmosphere during use, servicing, repair, and vehicle end of life [*Clodic et al.*, 2005; *Kuijpers*, 2011]. *Wimberger* [2010] took HFC-134a samples from vehicles on dismantler lots in California and found that on average only 27% of the initial HFC-134a remained in the mobile air-conditioning system before dismantlement, meaning that 73% had been released into the atmosphere.

Very large uncertainties remain in the inventory-based quantification of global and regional HFC-134a emissions [*Barletta et al.*, 2011], due to the diversity of emission processes and consumption habits [*Clodic et al.*, 2005; *Atkinson et al.*, 2003; *Rugh et al.*, 2004]. For instance, estimations of the HFC-134a emission rate from traffic [*Wallington et al.,* 2008] and domestic sector suffer from large uncertainties. The usage of HFC-134a for air conditioning varies not only with climate but also with region-specific equipment rate of air-conditioning systems in cars or national commitments within the United Nations Framework Convention for Climate Change (UNFCCC).

In this context, attempts have been made to deduce HFC-134a emission maps from HFC-134a atmospheric mole fraction measurements by statistical top-down methods. *Stohl et al.* [2009] developed their own global gridded HFC-134a emission inventory based on UNFCCC reporting and optimized it from atmospheric measurements using an inverse procedure and a Lagrangian transport model for years 2005 and 2006. Other studies focused on subcontinental regions: the U.S. [*Millet et al.*, 2009; *Manning and Weiss*, 2007; *Hu et al.*, 2015], Europe [*Keller et al.*, 2012], and East Asia [*Stohl et al.*, 2010; *Kim et al.*, 2010]. Some disagreements exist between these top-down estimates: *Stohl et al.* [2009] found that U.S. emissions in 2006 were 53% higher than the estimate of *Manning and Weiss* [2007] (28 Gg and 43 Gg, respectively). *Stohl et al.* [2009] also significantly increased the estimate made in the (Emissions Database for Global Atmospheric Research) EDGAR-v4.0 inventory (source: EC-JRC/PBL, http://edgar.jrc.ec.europa.eu/, 2010) for Chinese emissions in 2005. These various studies were restricted to short periods: years 2005–2006 for *Stohl et al.* [2009] and year 2008 for *Stohl et al.* [2010]. Therefore, they could not assess the global and regional emission growth rates since the enforcement of the Montreal Protocol in 1994 (Copenhagen Amendment).

This study aims to evaluate the evolution of HFC-134 emissions to the Montreal Protocol at the global and regional scales as seen from atmospheric measurements over the period 1995–2010.

The atmospheric inverse system includes a global chemistry transport model at a resolution of 3.75° × 2.5°. This allows the assessment of HFC-134 surface fluxes at the grid resolution, at an 8 day frequency, with a simultaneous optimization of OH concentrations in four latitudinal bands. Details on the inverse system and on the methodology are given in section 2. The inferred fluxes are analyzed in section 3 in terms of global and regional trends as well as seasonal variability.

2. Methodology

Our strategy follows the one applied by *Fortems-Cheiney et al.* [2013] for the study of HCFC-22 emissions. In our inverse system, a state vector **x**, representing the emissions, is optimized in order that both the distance between the atmospheric observations **y** and the simulated concentrations $H(\mathbf{x})$, and the distance between **x** and a prior knowledge on the emissions $\mathbf{x_b}$, are minimized given the respective uncertainties of **y** and $\mathbf{x_b}$. Their error covariance matrices **R** and **B**, respectively, represent these uncertainties. The Bayesian cost function J defined below is minimized iteratively and provides a solution, called posterior in the following.

$$J(\mathbf{x}) = (\mathbf{x} - \mathbf{x_b})^T \mathbf{B}^{-1} (\mathbf{x} - \mathbf{x_b}) + (H(\mathbf{x}) - \mathbf{y})^T \mathbf{R}^{-1} (H(\mathbf{x}) - \mathbf{y})$$

The minimization is performed by the M1QN3 limited-memory quasi-Newton minimization algorithm [*Gilbert and Lemaréchal*, 1989] and exploits the adjoint operator of H. We reduce the norm of the gradient of J by more than 99%.

Table 1. Global and Regional HFC-134a Emissions Before the Inversion (Prior) and After the Inversion (Posterior) in Gg/yr Over the Period 1995–2010[a]

	USA		Europe		Japan		China		Globe	
	Prior	Post	Prior	Post	Prior	Post	Prior	Post	Prior	Post
1995	10 ± 4	10 ± 2	4 ± 1	4 ± 1	4 ± 1	2 ± 1	<1	<1	20 ± 4	18 ± 2
1996	16	17	7	7	4	4	<1	<1	33	33
1997	22	23	9	9	5	6	<1	<1	43	44
1998	29	31	12	13	7	8	<1	<1	55	60
1999	37	35	15	16	8	9	<1	<1	71	70
2000	44	36	18	18	10	10	2	2	86	78
2001	50	42	21	20	11	11	2	2	98	89
2002	55	47	23	23	12	12	3	3	109	102
2003	59	50	26	25	13	13	5	5	121	110
2004	64	54	29	28	14	12	7	7	133	119
2005	68 ± 24	57 ± 9	30 ± 9	29 ± 5	15 ± 8	13 ± 4	9 ± 3	9 ± 2	145 ± 29	128 ± 5
2006	73	55	33	30	16	12	12	11	157	130
2007	77	61	35	31	16	12	15	14	170	138
2008	81	60	37	34	17	12	20	18	183	147
2009	81	59	37	34	17	11	20	18	183	147
2010	81 ± 29	71 ± 11	36 ± 11	37 ± 6	17 ± 11	12 ± 2	21 ± 8	20 ± 4	183 ± 34	167 ± 5

[a]As a trade-off between computing resources and completeness, we only estimate the posterior 1 sigma uncertainty for the years 1995, 2005, and 2010.

H represents the chemistry transport model and the nonlinear observation operator. The transport model is the offline version of the atmospheric general circulation model LMDz [*Hourdin et al.*, 2006]. The main sink of HFC-134a in the troposphere is its reaction with the radical hydroxyl OH: $CH_2FCF_3 + OH \cdot \rightarrow CHFCF_3 + H_2O$. The chemical scheme coupled to LMDz represents only the interaction between the radical hydroxyl OH and HFC-134a, and the other sinks are neglected. We use the reaction rate $k = 1.05 \times 10^{12} \exp(1630/T)$ $cm^3 \, molecule^{-1} \, s^{-1}$, as recommended by *Sander et al.* [2011]. The OH distribution is also optimized by the inverse system. The prior OH 3-D fields result from a simulation with full chemistry of the model LMDz-INtéractions Chimie et Aérosols [*Hauglustaine et al.*, 2004].

As a result, our state vector **x** includes (1) HFC-134a initial concentrations for 1 January 1995 at 00:00 at the model resolution (3.75° × 2.5° in longitude, latitude) and (2) HFC-134a surface emissions at an 8 day and at 3.75° × 2.5° resolution, for the 1995–2010 period—four factors to scale the OH prior atmospheric concentrations at an 8 day resolution, for four latitude bands (90°S–30°S, 30°S–0°, 0°–30°N, 30°N–90°N).

2.1. Prior Setup

Our gridded HFC-134a prior emissions in **x_b** are mostly taken from the EDGAR-v4.2 inventory (source: EC-JRC/PBL, http://edgar.jrc.ec.europa.eu/, 2011), which provides yearly estimates until 2008. We adapted this prior source specifically for China following *Stohl et al.* [2010]. Indeed, the small HFC-134a emissions in China (ranging from 0 in 1995 to about 1 Gg in 2008) suggested by the EDGAR-v4.2 inventory is not consistent with (1) the large development of air-conditioning systems in Chinese vehicles and (2) the ban of CFC-12 production in this country since the end of year 2010.

Hu et al. [2009], using an inventory-based approach, estimated that the Chinese HFC-134a emissions from automobile (including cars, bus, and trucks) air conditioners have increased from 7.3 Gg/yr in 2005 to 21.2 Gg/yr in 2010. Applying a growth rate of 23%/yr of mobile air conditioners from 1995 to 2010 and assuming that automobile air conditioners account for two thirds of total HFC-134a emissions like *Stohl et al.* [2010], we obtain prior Chinese HFC-134a emissions ranging from less than 1 Gg/yr in 1995 to 21 Gg/yr in 2010 (see Table 1).

For the rest of the world, we made no effort to adjust the EDGAR-v4.2 inventory to the years 2009 and 2010 in the prior. Figures 1a and 1e displays the grid point prior emissions in 1995 and 2010. Whereas HFC-134a emissions are mostly localized around industrial sites in Europe (Benelux), in the USA (Silicon Valley, California; Silicon Prairie, Texas; Research Triangle, North Carolina; and Route 128, Massachusetts), and in Japan in 1995, large emissions are less localized but more spatially distributed over these continents in 2010. A broader distribution of HFC-134a emissions is also supported by the inversion analysis of atmospheric data provided in *Hu et al.* [2015].
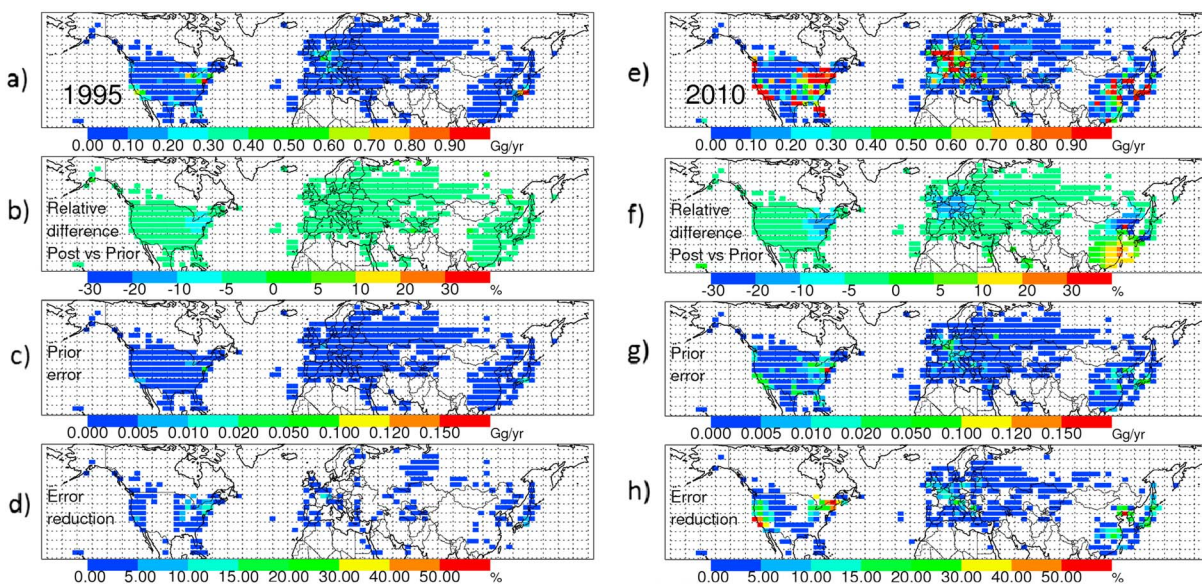
Figure 1. (a) Grid point prior HFC-134a emissions in Gg/yr for year 1995. (b) Relative difference between posterior and prior emissions in %. (c) Prior uncertainty in Gg/yr. (d) Uncertainty reduction at the grid point resolution, in %. (e–h) Same as Figures 1a–1d, but for year 2010.

The grid point standard deviations of the prior errors assigned to the HFC-134a prior emissions are set at 100% of the flux. Prior error correlations in space are represented by an *e*-folding length of 500 km over land and temporal correlation by an *e*-folding length of 8 weeks. These prior error statistics lead to annual global HFC-134a budgets of 20 ± 4 Gg/yr for year 1995 and of 183 ± 34 Gg/yr for year 2010 (from now on, the plus-minus signs represent the 1 sigma standard deviation), leading to a large 20% 1 sigma uncertainty. The resulting prior error uncertainty is $\pm 30\%$ for Europe and about $\pm 35\%$ for the U.S. and China, which fairly represents the large and uncertain interannual variability of the regional HFC-134a emissions in recent years.

The errors assigned to the scaling factors of OH are of 10% (1 sigma), based on the differences between various estimates of OH concentrations [*Prinn et al.*, 2001; *Krol and Lelieveld*, 2003; *Bousquet et al.*, 2005].

2.2. Assimilated Observations

Our observation data set includes measurements of HFC-134a dry air mole fractions made at 21 sites, listed in Table 2, from December 1994 to March 2011. It was downloaded from the World Data Center for Greenhouse Gases (http://ds.data.jma.go.jp/gmd/wdcgg/, accessed 15 November 2012), except for the Gosan data. We use both flasks (from the NOAA/Earth System Research Laboratory (ESRL) [*Montzka et al.*, 1996; *Montzka et al.*, 2014] and from the Italian National Agency for New Technologies, Energy and Sustainable Economic Development (ENEA) [*Artuso et al.*, 2010] networks) and continuous measurements (from the Advanced Global Atmospheric Gases Experiment (AGAGE) [*Prinn et al.*, 2000; *O'Doherty et al.*, 2004] and from the National Institute for Environmental Studies (NIES) networks [*Yokouchi et al.*, 2006]), respectively, named "event" and "daily" data in the database. Continuous measurements by the AGAGE and NIES networks were averaged over daytime, and these daily means were used as constraints together with the flask measurements. The total number of observational constraints for the entire period is 17,803.

The different stations are sparsely distributed over the globe but mainly located in the Northern Hemisphere (Figure 2). Before 1998, there were mainly flask measurements available, leading to a small number of HFC-134a observational constraints (129 in 1997). After 1998, some continuous measurements were made gradually available, so that 643 constraints were used in 2003 and 2246 in 2007. The evolution of the total number of observational constraints used in the inversion per year is shown in Figure 3 for the regions USA, Europe, and China, where most of the stations are located. Note that measurements of HFC-134a over the continental U.S. beginning in 2008 recently became available [*Hu et al.*, 2015] but are not included in this analysis.

The estimate of all the errors involved in the observation errors in the inversion system, defined as in *Fortems-Cheiney et al.* [2013], is approximately 3% (mean value of 1.3×10^{-6} ppm). It combines representation errors

Table 2. List of the Stations Performing HFC-134a Measurements Used in This Study[a]

Station	Code	Latitude (deg)	Longitude (deg)	Altitude (meters above sea level)	Network	Type	Sampling Frequency	Data Period
Alert, Canada	ALT	82.50	−62.30	210	NOAA	flask	weekly	12/1994–03/2011
Point Barrow, AK, USA	BRW	71.30	−156.60	11	NOAA	flask	weekly	12/1994–03/2011
Cape Grim, Tasmania	CGO	−40.68	144.68	104	AGAGE	continuous	hourly	01/1998–03/2011
Cape Grim, Tasmania	CGO	−40.68	144.68	21	NOAA	flask	weekly	12/1994–03/2011
Cape Ochi-ishi, Japan	COI	43.15	145.50	96	NIES	continuous	hourly	08/2006–12/2010
Gosan, South Korea	GOS	33.17	126.90	46.5	AGAGE	continuous	hourly	11/2007–03/2011
Hateruma, Japan	HAT	24.05	123.80	46.5	NIES	continuous	hourly	05/2004–12/2010
Harvard Forest, USA	HFM	42.90	−72.30	340	NOAA	flask	weekly	11/1995–03/2011
Jungfraujoch, Switzerland	JFJ	46.54	7.98	3580	AGAGE	continuous	hourly	01/2000–03/2011
Cape Kumakahi, HI, USA	KUM	19.52	−154.82	3	NOAA	flask	weekly	11/1995–03/2011
Park Falls, WI, USA	LEF	45.92	−90.27	868	NOAA	flask	weekly	10/1996–03/2011
Lampedusa, Italy	LMP	35.52	12.63	45	ENEA	flask	weekly	12/2003–12/2008
Mace Head, Ireland	MHD	53.33	−9.90	25	AGAGE	continuous	hourly	12/1994–03/2011
Mace Head, Ireland	MHD	53.33	−9.90	8	NOAA	flask	weekly	10/1998–03/2011
Mauna Loa, USA	MLO	19.54	−155.58	3397	NOAA	flask	weekly	12/1994–03/2011
Palmer Station, Antarctica	PSA	−64.92	−64.00	10	NOAA	flask	weekly	12/1997–03/2011
Ragged Point, Barbados	RPB	13.17	−59.43	42	AGAGE	continuous	hourly	05/2005–03/2011
Cape Matatula, Samoa	SMO	−14.24	−170.57	77	AGAGE	continuous	hourly	05/2006–03/2011
Cape Matatula, Samoa	SMO	−14.24	−170.57	42	NOAA	Flask	weekly	12/1994–03/2011
South Pole, USA	SPO	−89.98	−24.80	2810	NOAA	flask	weekly	12/1994–03/2011
Summit, Greenland	SUM	72.58	−38.48	3238	NOAA	flask	weekly	06/2004–03/2011
Tierra del Fuego, Argentina	TDF	−54.87	−68.48	20	NOAA	flask	weekly	05/2004–05/2010
Trinidad Head, CA, USA	THD	41.05	−124.15	120	NOAA	flask	weekly	03/2002–03/2011
Trinidad Head, CA, USA	THD	41.05	−124.15	140	AGAGE	continuous	hourly	03/2005–03/2011
Ny-Alesund, Norway	ZEP	78.90	11.88	474	AGAGE	continuous	hourly	01/2001–03/2011

[a]See Figure 2 for the station locations. The data period listed is specific to this study. The different networks are NOAA/ESRL, the National Oceanic and Atmospheric Administration, Earth System Research Laboratory; AGAGE, the Advanced Global Atmospheric Gases Experiment; NIES, the National Institute for Environmental Studies, and ENEA, the Italian National Agency for New Technologies, Energy and Sustainable Economic Development. The AGAGE data are 2-hourly for the newer Medusa-GCMS measurements and 4-hourly for the older ADS-MS measurements.

(e.g., the mismatch between the observation and model resolutions), errors of the observation operator (including transport and chemical-scheme errors in LMDz-SACS), measurements errors (including instrumental precision for HFC-134a measurements and the errors involved in the calibration scales), and errors of the Chemistry Transport Model (CTM). The measurements coming from AGAGE, NOAA, and NIES networks are, respectively, calibrated using SIO-2005, NOAA/Climate Monitoring and Diagnostics Laboratory, and NIES-2008 scales. It should be noted that differences between networks (calibrations uncertainties and intercalibration factors) are small [*Stohl et al.*, 2010; *Carpenter et al.*, 2014], compared to other causes of uncertainties
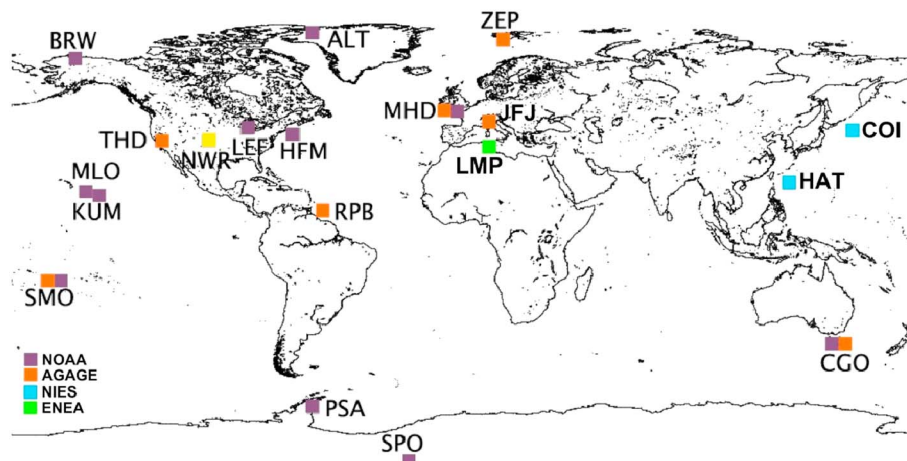

Figure 2. Locations of the stations measuring HFC-134a dry air mole fractions used in the inversion. The measurements of the Niwot Ridge station (NWR, USA) displayed in yellow are only used for the evaluation.
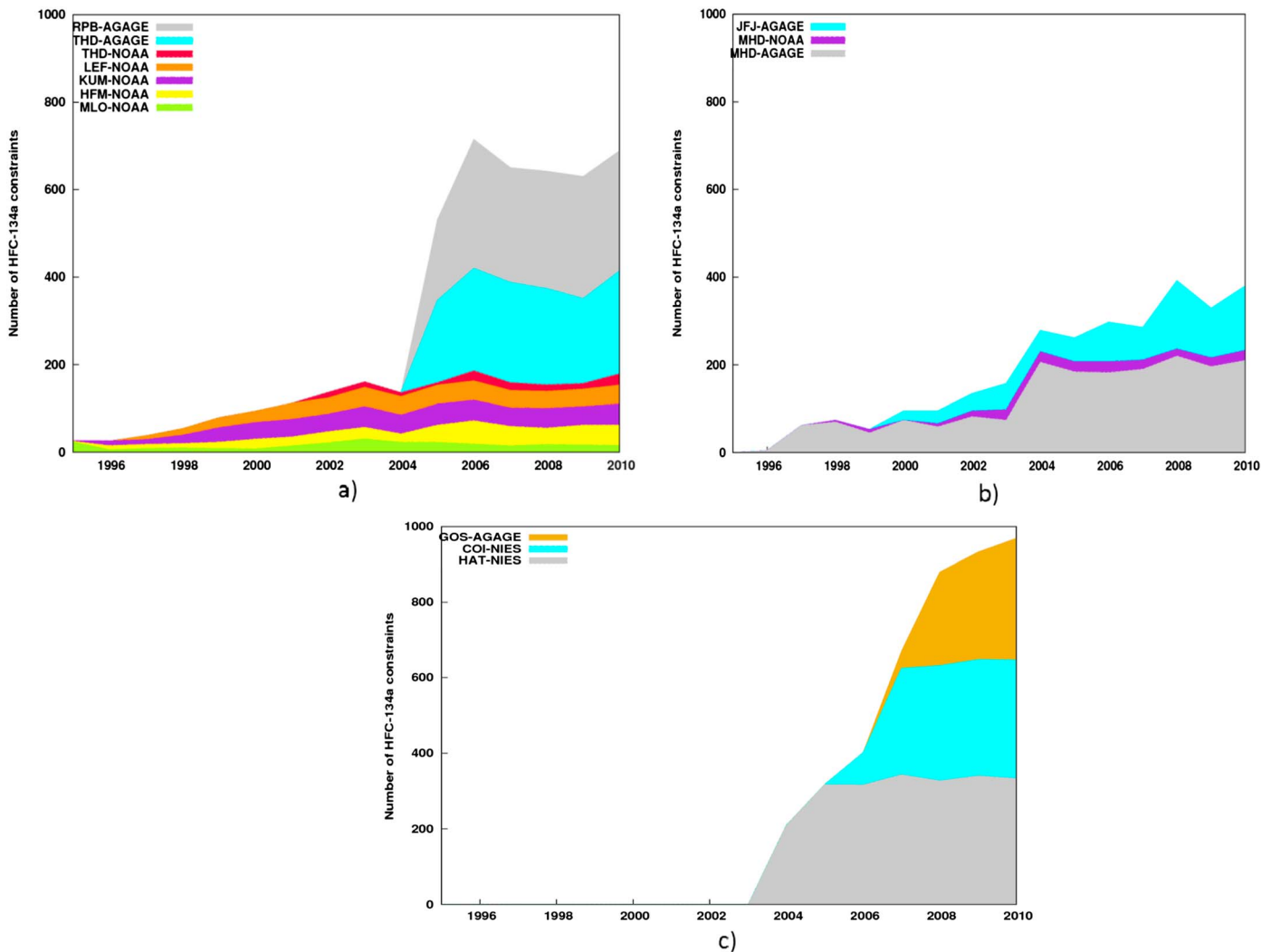
Figure 3. Total number of HFC-134a constraints used in the inversion system per year for (a) the U.S., (b) Europe, and (c) China. See Figure 2 for the locations of the stations.

such as representation or model errors. Error correlations between the measurements are neglected, so that the covariance matrix R of the observation errors is diagonal (i.e., only variances are taken into account). It should be noted that the degree of freedom of the inverse problem is about 255.

2.3. Calculation of the Analysis Error

The calculation of the analysis error is challenging in the framework of variational inverse system. Even though the analysis error covariance matrix can be written in various analytical forms, it requires the inversion of matrices that are too large to invert given the current computational resources in our variational approach. As a result, one way to compute the analysis error is to perform a randomization approach (Monte Carlo) to estimate the posterior errors on the fluxes. The result of this method is in agreement with the Bayesian covariance matrix A. This approach has been described in *Chevallier et al.* [2007] and contains the following steps: (1) running the LMDz-SACS chemistry-transport model with a climatology of surface emissions to generate a set of pseudo HFC-134a observations at the same location and time as the actual measurements, (2) perturbing the pseudoobservations consistently with assumed observation error statistics (described later in the section), (3) perturbing the state vector (that includes the surface flux climatology) consistently with assumed error statistics, (4) performing a Bayesian inversion of the surface fluxes using the perturbed pseudoobservations as constraints and perturbed state vector as the prior field, and (5) comparing the estimate of the inversion to the flux climatology to get the Bayesian errors of the estimate.

Table 3. Regional and Global Uncertainty Reductions in %, for the Years 1995, 2005, and 2010

	USA	Europe	Japan	China	Globe
1995	54	-	11	-	56
2005	56	45	40	23	71
2010	61	45	80	46	84

The method is applied 10 times with different perturbations each time, in order to compute the posterior error statistics. We estimate the posterior 1 sigma uncertainty from these Monte Carlo inversion ensembles (10 members) for three different years: 1995, 2005, and 2010. Following the usual practice, we define the uncertainty reduction as $(1 - \sigma_a/\sigma_b) \times 100$, with σ_b the prior error standard deviation and σ_a the theoretical posterior error standard deviation.

3. Results

3.1. Theoretical Performance of the Inversion

The uncertainty on the posterior emissions, calculated with the Monte Carlo approach, is presented in Table 1 for the years 1995, 2005, and 2010. The uncertainty reductions reached by the inversion for the years 1995, 2005, and 2010 are synthesized in Table 3 for regional and global aggregations. The uncertainty reduction at the grid-scale resolution is also shown in Figures 1d and 1h, respectively, for years 1995 and 2010. In 1995, the global uncertainty reduction reaches 56%. At the regional scale, the uncertainty associated with the emissions is reduced by 54% for the U.S. and 11% for Japan. However, the uncertainty reduction remains small for Europe and China, owing to the lack of sampling locations near these regions (Table 2).

The expansion of the surface network increases the number observational constraints in the inversion over time. Combined with the increased emissions in the atmosphere, this leads to larger uncertainty reductions, as shown in Figure 1 and in Table 3, both at the global (71% and 84% in 2005 and in 2010) and at regional scales. Indeed, in 2005, the uncertainty reduction is 56% for the U.S. and 45% for Europe. For Japan and China, the uncertainty reduction is 40% and 23%; this increase of uncertainty reduction coincides with the setup of the first Asian site, Hateruma, in May 2004. Thanks to the benefits of the sites Gosan in South Korea (since November 2007) and Cape Ochi-ishi in Japan (since August 2008), the uncertainty reduction reaches 81% and 46%, respectively, in 2010.

3.2. Global HFC-134a Emissions

Table 1 presents the annual global prior and posterior HFC-134a emissions. Figures 1b and 1f show the relative difference between posterior and prior HFC-134a emissions at the grid point resolution, respectively, in 1995 and in 2010. Figures 4 and 6 show the global posterior HFC-134a emissions. Posterior emissions range from 18 ± 2 Gg/yr in 1995 to f167 ± 5 Gg/yr in 2010 (see Table 1 and Figure 4). These estimates are in excellent agreement with the posterior emissions of *Xiang et al.* [2014], ranging from 20 Gg in 1995 to 153 Gg in 2010 who used the same NOAA and AGAGE networks and additional observational data (i.e., the aircraft campaigns Hiaper-Pole-to-Pole of Carbon Cycle and Greenhouse Gases Study HIPPO over the Pacific Ocean) to derive global emissions for these years. As seen in Table 1, this is also consistent with the posterior emissions of *Montzka et al.* [2014] and *Rigby et al.* [2014], ranging, respectively, from 22 Gg in 1995 to 168 and 167 Gg in 2010.

It is interesting to see that the yearly increase we derive is more pronounced from 2009 to 2010 (growth rate of +14%) than from 2005 to 2009 (mean growth rate of 3.5%). The absolute global emission magnitudes and increase in emissions are also consistent with the +17% inferred by *Lunt et al.* [2015] between their average estimate of 141.6 Gg/yr for the 2007–2009 period and of 166.5 Gg/yr for the 2010–2012 period (derived with 10 measurement stations from AGAGE and NIES networks).

One should note that discrepancies between different global-based inverted results can be due to the observational measurements used to constrain the emissions but also to the diversity of the inversion systems (such as the CTM used, whether or not the OH fields are prescribed in the model). Nevertheless, all these independent studies show a continuous rise of HFC-134a emissions between 1995 and 2010.
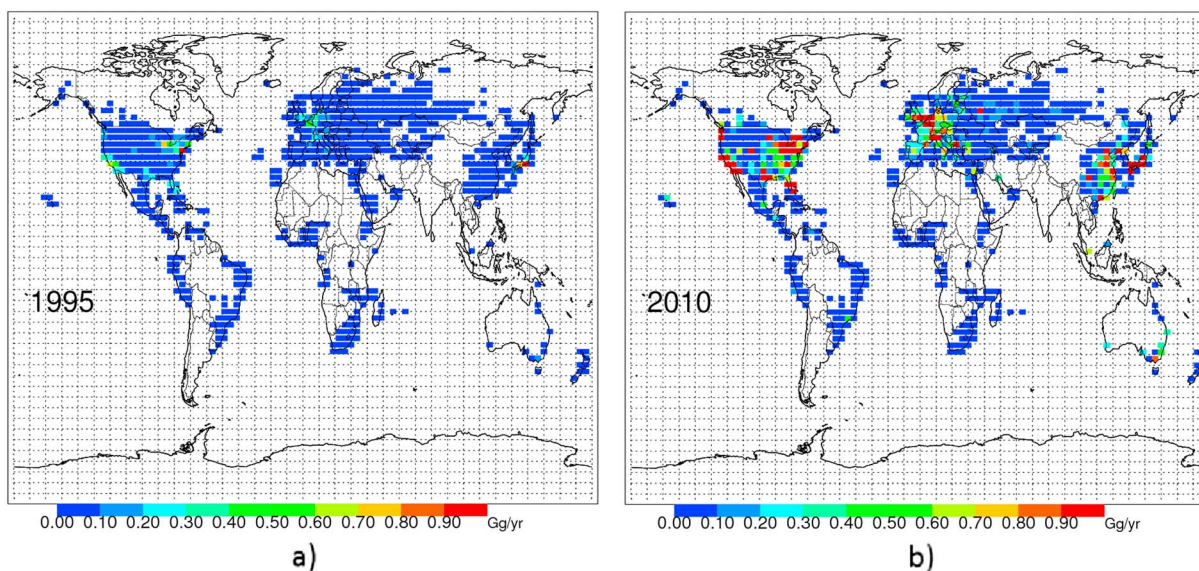
Figure 4. Grid point global posterior HFC-134a emissions in Gg/yr for (a) year 1995 and (b) year 2010.

Until the year 2000, posterior estimates are smaller than the prior ones with relative differences of about −4%. The differences between the prior and the posterior estimates increase after 2000 (i.e., −13% in 2005), demonstrating an overestimation of the EDGAR-v4.2 HFC-134a emissions on global scale.

3.3. Regional HFC-134a Emissions and Growth Rates

Almost all the posterior regional estimates are smaller than the prior ones: −7% for the U.S., especially over the east coast (modification in a range of −10% to −20%); −8% for Europe; and −23% for Japan in 2010. On the contrary, the Chinese posterior estimate is about the same as the prior one. In the following, regional HFC-134a emissions are discussed in details for the U.S., Europe, China, and Japan.

3.3.1. The United States of America Emissions

The posterior inventory highlights the U.S. as the main HFC-134a source, contributing at least 45% of the global emissions since 1995.

Our posterior U.S. emissions are higher than most of the previous studies for the years 2005–2007 (see Table 4). In 2005, we infer emissions 62% higher (57 ± 9 Gg/yr, starting from a prior of 68 ± 24 Gg/yr) than the 35 Gg/yr of *Stohl et al.* [2009] (starting from a prior of 57 Gg/yr). Our posterior U.S. estimates are also more than 2 times larger than the HFC-134a emissions estimated from aircraft measurement campaigns in 2004 and 2006 by *Millet et al.* [2009] and higher than the estimates of 43 Gg/yr (22–60) of *Manning and Weiss* [2007] for year 2006 and of 43 ± 6 Gg/yr of *Barletta et al.* [2011] for 2008. The more comprehensive suite of data used here compared to these studies (e.g., measurements only from the THD stations for *Manning and Weiss* [2007]) may explain such differences. On the contrary, our 2008–2010 average of 63 ± 9 Gg is in good agreement with the 52–61 Gg average estimated by *Hu et al.* [2015] for 2008–2010, derived from multiple inversion scenarios and using data from more sites (with daily flasks air samples and aircraft campaigns) over the U.S. than in our study.

As shown in Figures 4 and 7, our estimate for the U.S. shows a progressive increase between 1995 and 2010, ranging from 10 ± 2 Gg/yr (starting from a prior of 10 ± 4 Gg/yr) to 71 ± 11 Gg/yr (starting from a prior of 81 ± 29 Gg/yr). The U.S. emission growth rate nevertheless slows down, from +33%/yr between 1995 and 2000 to +7.5%/yr between 2000 and 2005 and to +5%/yr between 2005 and 2010. Until year 2006, our estimates are in excellent agreement with the Environmental Protection Agency (EPA) estimates (i.e., 54 Gg/yr against 57 Gg/yr, respectively, for the year 2004) [*EPA*, 2008]. However, our estimated HFC-134a emission increase from 2006 to 2010 contrasts with the decrease suggested by the EPA estimates for these years [*EPA*, 2014].

It also should be noted that the posterior emissions show a slight decrease in 2009, also seen by *Hu et al.* [2015], which is consistent with the decrease of number of vehicles per thousand people (828)

Table 4. Comparison With Previous Published Annual Total Budgets for the Period 1995–2010 Studied Here

Globe	Literature	This Work
1996	20 [*Xiang et al.*, 2014]	17
2007–2009	141.6 [*Lunt et al.*, 2015]	144
2010	153 [*Xiang et al.*, 2014]	167
	U.S.	
2004	27 [*Millet et al.*, 2009]	54
2005	35 [*Stohl et al.*, 2009]	57
2006	43 [*Manning and Weiss*, 2007]	55
2008	43 ± 6 [*Barletta et al.*, 2011]	60
2008	53–70 [*Hu et al.*, 2015]	60
2009	47–60 [*Hu et al.*, 2015]	59
2010	54–68 [*Hu et al.*, 2015]	71
	Europe	
2000–2002	23.6 [*Reimann et al.*, 2004]	20
2000–2002	10 [*O'Doherty et al.*, 2004]	20
2005	24 [*Stohl et al.*, 2009]	29
2006	27 [*Stohl et al.*, 2009]	30
	China	
2004–2005	3.9 ± 2.4 [*Yokouchi et al.*, 2006]	8
2005	8.7 [*Kim et al.*, 2010]	9
	9.8 [*Stohl et al.*, 2009]	
2010	6 ± 5.6 [*Yao et al.*, 2012]	21
	Japan	
2002	4.4 [*Yokouchi et al.*, 2006]	11
2005	5.3 [*Stohl et al.*, 2009]	13
2006	4 [*Stohl et al.*, 2009]	12

[*U.S. Department of Transportation,* 2012] and with the decrease of fossil fuel CO_2 emissions from transportation [*U.S. Energy Information Administration*, 2014], probably due to the economic recession. However, this interannual variability for the years 2008–2010 with decrease in 2009 and upwelling in 2010 is not reproduced by the EPA estimates [*EPA*, 2014].

3.3.2. Europe

The European prior budget is smaller than the U.S.'s (68 Gg/yr against 30 Gg/yr in 2005, see Table 2), even though the European number of vehicles is higher (for example, 253 millions against 275 millions in 2005 in Europe, estimated with the World Bank http://www.worldbank.org/, and *Davis et al.* [2012] data). This can be explained by a higher HFC-134a demand for the mobile air-conditioning sector in the U.S. compared to Europe: when the equipment rate of air-conditioned systems in newer vehicles was 95% for the USA in 1995, it was only 35% for Europe (and then almost 90% in 2005) [*Saba et al.*, 2009; *Barbusse and Gagnepain*, 2003]. The U.S./Europe difference can be also explained by the use in Europe of another gas for the domestic refrigeration, HC600a (isobutane, $(CH_3)_3CH$), which is not used in the U.S. due to flammability issue [*Saba et al.*, 2009].

Our European posterior emissions are in a good agreement with *Stohl et al.* [2009] and with *Reimann et al.* [2004] (see Table 4). However, our European budget is twice higher than the estimates of *O'Doherty et al.* [2004], with 20 Tg compared to 10 Tg for the years 2000–2002, respectively. However, it should be noted that their study had only benefited from the Mace Head station (compared to the use of the additional JFJ station here).

3.3.3. China

Our posterior Chinese emissions of 8 ± 3 Gg/yr (starting from a prior of 8 ± 2 Gg/yr) are higher than the estimates of *Yokouchi et al.* [2006] for the years 2004–2005 and also significantly higher than the estimates of *Yao et al.* [2012] for the year 2010 (see Table 4). However, our posterior Chinese estimates of 9 ± 3 Gg/yr (starting from a prior of 9 ± 2 Gg/yr) is similar to the 8.7 Gg/yr (6.5–12) of *Kim et al.* [2010] and to the 9.8 Gg/yr of *Stohl et al.* [2009] for year 2005. With a growth rate of 22%/yr (in agreement with the +20%/yr obtained by *Stohl et al.* [2010] between 2005 and 2006), the Chinese emissions reach 11 Gg/yr in 2006.

With a 2005–2010 mean growth rate of +20%/yr, the Chinese emissions reach 18 Gg/yr in 2008, 40% higher than the 12.9 ± 1.7 Gg estimates of *Stohl et al.* [2010]. Our Chinese emissions of 20 ± 4 Gg in 2010 are also

higher 63% higher than the estimates of *Lunt et al.* [2015] for this year, derived from a different set of observational constraints (from eight AGAGE and two NIES measurement stations). Nevertheless, our 2010 Chinese value of 20 ± 4 Gg is consistent with the estimates of *Su et al.* [2015] that suggest about 17 Gg of HFC-134a from mobile air conditioning only, using an improved bottom-up method.

3.3.4. Japan

Our Japanese posterior emissions are lower than the prior ones after year 2003, indicating an overestimation of EDGAR-v4.2 inventory during the period 2004–2010. These posterior emissions are significantly higher than the previous estimates published in the literature. For instance, for the year 2002, we derive posterior Japanese emissions of 11 Gg/yr in 2002 substantially higher than the 4.4 Gg/yr found by *Yokouchi et al.* [2005]. For 2005 and 2006, we find posterior emissions of 13 ± 4 Gg/yr and 12 Gg/yr for 2005 and 2006 also higher than the 5.3 and 4.0 Gg/yr of *Stohl et al.* [2009] for the same years. It is worth noting that substantial differences exist between inventory-based quantifications of the Japanese HFC-134a emissions: the EDGARv4.2 inventory estimates the Japanese emissions at 15 ± 8 Gg/yr in 2005, while the UNFCCC (United Nations Framework Convention on Climate Change) suggests 3.5 Gg/yr. For their study, *Stohl et al.* [2009] used the UNFCCC inventory as prior, while we use EDGARv4.2. The differences in the choice of prior may be critical, especially if the uncertainty associated to the prior is not well defined and prevents the system from a potentially necessary but important departure from the prior.

3.4. Evaluation Against Independent Measurements

To evaluate our posterior HFC-134a U.S. emissions, we compared model simulations with the independent (i.e., not used as constraints in the inversion) HFC-134a measurements from two campaigns: ARCTAS (Arctic Research of the Composition of the Troposphere from Aircraft and Satellites, NASA project, [*Barletta et al.*, 2011]) and CalNex (California Research at the Nexus of Air Quality and Climate Change, [*Barletta et al.*, 2013]). The ARCTAS air samples were obtained on board research flights (DC-8) that flew over California during June 2008. The CalNex 2010 study was performed during May to June 2010. Air samples were collected on board a National Oceanic and Atmospheric Administration (NOAA) WP-3D aircraft. Particular emphasis was placed on three large source regions—the South Coast Air Basin, the Sacramento Valley, and the San Joaquin Valley—with almost 80% of the samples collected at altitudes below 2 km over the South Coast Air Basin of California and the Central Valley [*Barletta et al.*, 2013].

We have computed bias and root-mean-square error between the modeled and observed HFC-134a concentrations for each of the 164 and 1125 data, respectively, for ARCTAS and CalNex, before and after inversion. In Figure 5, we present ratios between prior and posterior mean bias and root-mean-square error at the grid cell scale. For bias, ratio has been calculated as

$$\text{Ratio} = \frac{\text{independent measurement} - \text{model (before inversion)}}{\text{independent measurements} - \text{model (after inversion)}}$$

Grid cells in green, corresponding to a ratio lower than 1, indicate an improvement of the corresponding statistical indicator after optimization.

To further evaluate the interannual variability of our posterior HFC-134a emissions over the long period 1995–2010, we also used cross-validation technique by removing the Niwot Ridge station (from the NOAA network) from the inversion, and we performed an independent evaluation with this site. Figure 8 shows that the inversion leads to a significant improvement relative to the prior simulation. The mean annual reduction of the bias indeed ranges from −13% in 1995 to −80% in 2010, allowing us to confirm that American HFC-134a emissions are overestimated in the EDGAR-v4.2 inventory used here as prior, as seen by *Hu et al.* [2015]. This overestimation is particularly pronounced after year 2002.

3.5. Seasonality

The 8 day resolution of our inversion reveals seasonal variations in the posterior emissions (which are not present in the prior estimates; see Figures 6 and 7). A seasonal cycle is inferred by the inversion, comparable to the seasonality found by *Xiang et al.* [2014] and by *Hu et al.* [2015]. It is interesting to note that this seasonality is similar to the one found by *Fortems-Cheiney et al.* [2013] and by *Xiang et al.* [2014] in HCFC-22 emissions. The seasonal variations of HFC-134a emissions, with higher emissions in summer than in winter, are driven by the U.S. and to a lesser extent by Europe and China. HFC-134a emissions may be exacerbated by higher needs
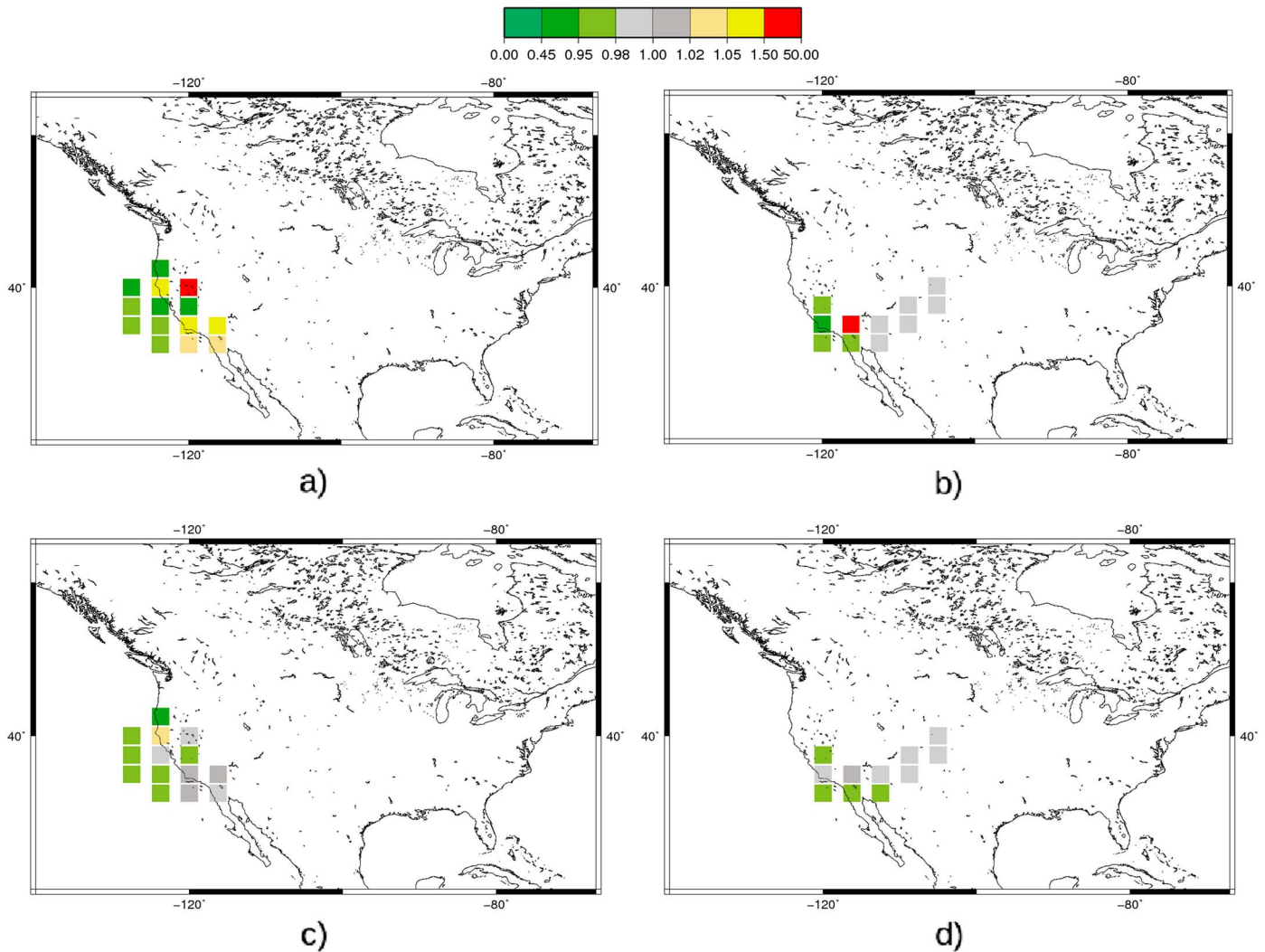
Figure 5. Ratio of the posterior to the prior values of the bias (in absolute value) between simulated and observed concentrations for (a) ARCTAS (flying in June 2008) and (b) CalNex (flying in May–June 2010) campaigns. Ratio of the posterior to the prior values of the root-mean-square error between simulated and observed concentrations for (c) ARCTAS and (d) CalNex. The inversion improves the simulation when the ratios are less than 1 (in green).
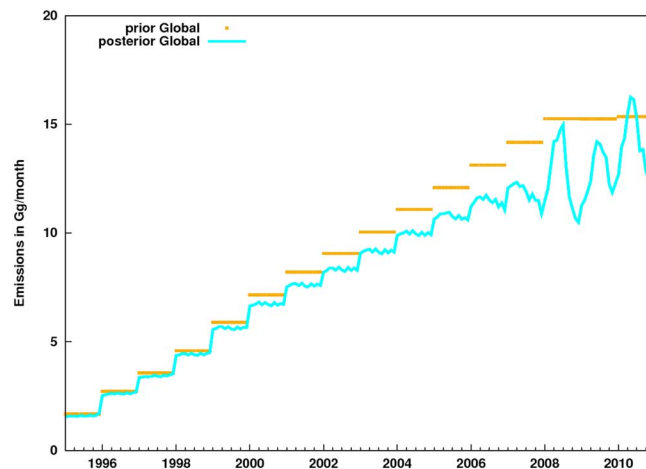

Figure 6. Global monthly HFC-134a prior and posterior emissions (in yellow and blue), from 1995 to 2010, in Gg/month.

of air conditioning during the warm period and also by extra leaks that occur during the maintenance of cooling systems [*Schwarz and Harnisch*, 2003].

U.S. emissions exhibit little seasonality prior to 2002 but show an apparent seasonal trend in subsequent years (+4% between January and July 2002, +10% between January and July 2006). This could be explained by (i) the increasingly strong signal associated to more than 95% of vehicles equipped with HFC-134a as refrigerant in 2005 [*Saba et al.*, 2009] and/or (ii) by the introduction of continuous in situ measurements (i.e., in 2005 at stations Trinidad Head and Ragged Point) and then by the increase
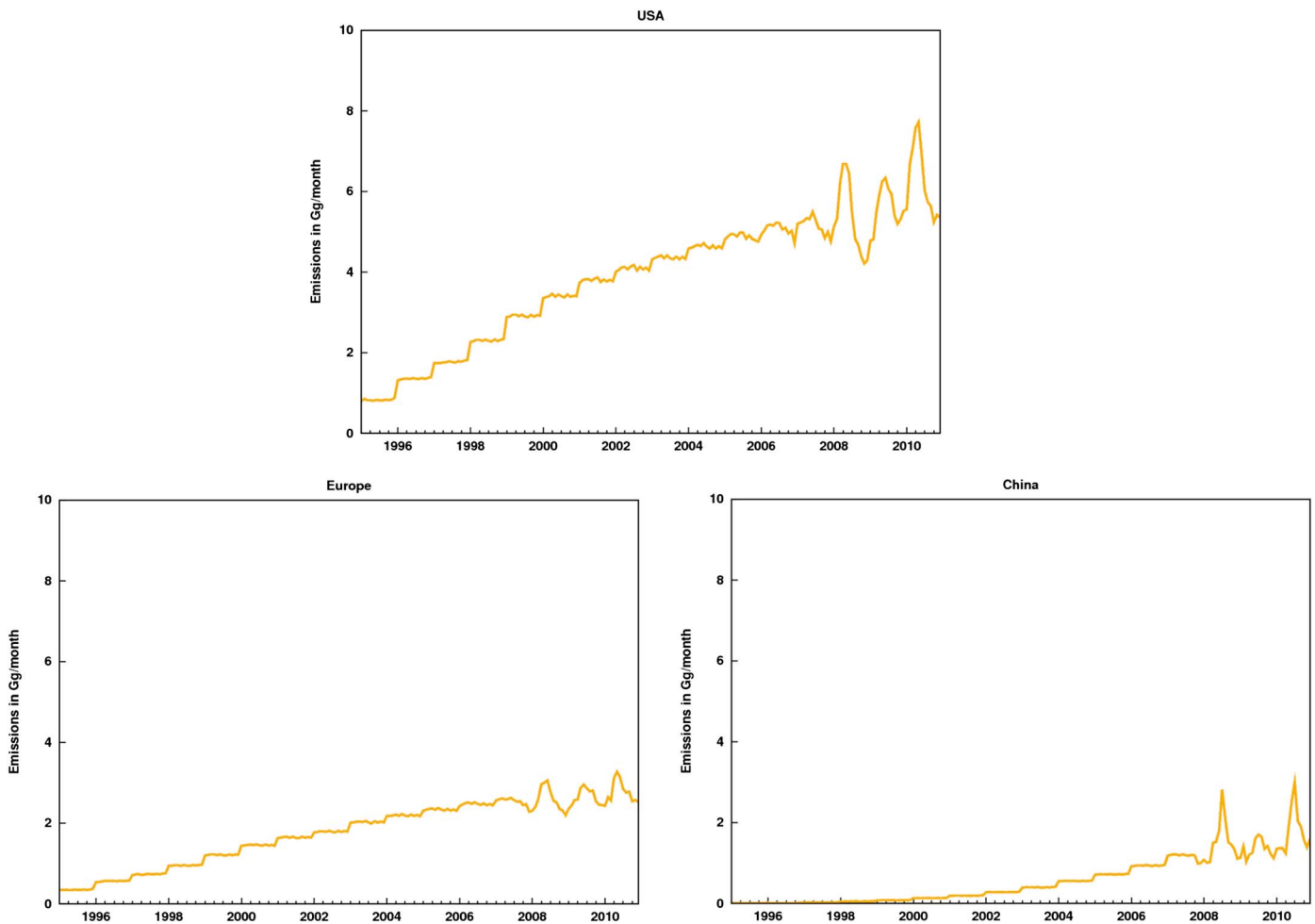
Figure 7. HFC-134a posterior emissions from 1995 to 2010, for the U.S., Europe, and China, in Gg/month.
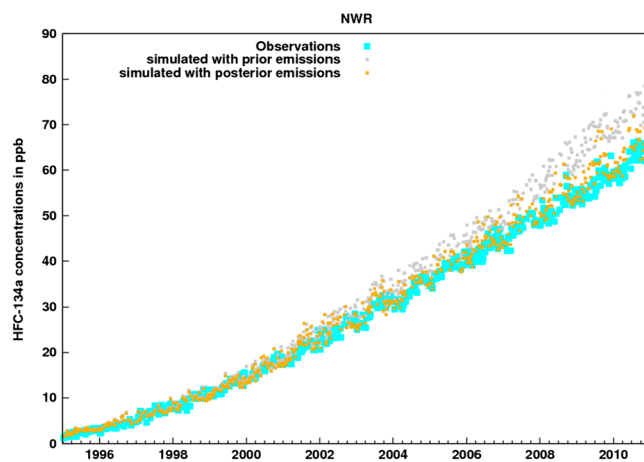

Figure 8. Simulated prior (grey) and posterior (yellow) compared to the measured (blue) HFC-134a concentrations at station Niwot Ridge (Colorado, USA). See Figure 2 for the station location. The mean annual reduction of the bias indeed ranges from −13% in 1995 to −80% in 2010.

of observational constraints that could allow the capture of such a signal.

After 2007 the seasonality of the U.S. emissions becomes strong. For example in 2008, the U.S. August emissions are 26% greater than the January ones (6.44 against 5.12 Gg/month, respectively). This results in a slight overestimation of the summer HFC-134a concentrations at NWR station (used for the independent evaluation, see section 3.4 and Figure 8). Nevertheless, such seasonality is also found by *Hu et al.* [2015], using different more constrained (with daily flask air samples and aircraft campaigns) inversion scenarios. They suggested that U.S. summer emissions are 20–50% greater than during winter for the 2008–2012 period.

4. Conclusions

We have estimated the spatial and temporal variability of HFC-134a emissions over 16 years, between 1995 and 2010, at a $3.75° \times 2.5°$ and at 8 day resolution, improving our knowledge of the HFC-134a emissions by optimizing both their amplitude and their seasonality.

One of the major findings of this study is the appearance of a seasonal cycle in the HFC-134a emissions in 2002, which becomes enhanced over time. Our results also suggest that the gridded EDGAR-v4.2 inventory overestimates the U.S. and the Japanese budget and confirm the large underestimation of Chinese emissions by this same inventory.

U.S. emissions, and to a lesser extent European emissions, appear to have drastically increased since 1995 (from 10 to 71 Gg/yr in 2010 and from 4 to 37 Gg/yr in 2010, respectively). Driven by these enhancements, the global HFC-134a emissions have reached the unprecedented level of 167 ± 5 Gg/yr in 2010.

However, the regional growth rates have slowed down since 1995 over developed countries, with a rate of +5%/yr for the U.S., +4%/yr for Europe, and near zero for Japan over 2005–2010. On the contrary, the Chinese emissions, although currently lower than U.S. and European emissions, appear to grow at a rate of +20%/yr since 2005. Due to the growing demand for vehicles in Asia (269 vehicles per thousand people in 2030 [*Davis et al.*, 2012; *WARD*, 2010]), the HFC-134a emissions could potentially continue to rise significantly in the near future [*Velders et al.*, 2009; *Su et al.*, 2015], unless this species is phased out by international agreements (e.g., Directive 2006/40/EC of the European Union or North American HFC phase-down amendment proposal [*EPA*, 2014]).

References

Artuso, F., P. Chamard, S. Chiavarini, A. di Sarra, D. Meloni, S. Piacentino, and D. M. Sferlazzo (2010), Tropospheric halocarbons and nitrous oxide monitored at a remote site in the Mediterranean, *Atmos. Environ.*, 44(38), 4944–4953.

Atkinson, W., J. A. Baker, and W. Hill (2003), Mobile air conditioning industry overview, 24 pp., SAE Interior Climate Control Standards Committee, Automotive Industry Executive Summit on Vehicle Climate Control, Society of Automotive Engineers (SAE), Troy, Mich., Feb.

Barbusse, S., and L. Gagnepain (2003), La climatisation automobile, impact énergétique et environnemental, Données et Références ADEME.

Barletta, B., P. Nissenson, S. Meinardi, D. Dabdub, F. Sherwood Rowland, R. A. VanCuren, J. Pederson, G. S. Diskin, and D. R. Blake (2011), HFC-152a and HFC-134a emission estimates and characterization of CFCs, CFC replacements, and other halogenated solvents measured during the 2008 ARCTAS campaign (CARB phase) over the South Coast Air Basin of California, *Atmos. Chem. Phys.*, 11, 2655–2669, doi:10.5194/acp-11-2655-2011.

Barletta, B., et al. (2013), Emission estimates of HCFCs and HFCs in California from the 2010 CalNex study, *J. Geophys. Res. Atmos.*, 118, 2019–2030, doi:10.1002/jgrd.50209.

Bousquet, P., D. Hauglustaine, P. Peylin, C. Carouge, and P. Ciais (2005), Two decades of OH variability as inferred by an inversion of atmospheric transport and chemistry of methyl chloroform, *Atmos. Chem. Phys.*, 5, 2635–2656, doi:10.5194/acp-5-2635-2005.

Carpenter, L. J., S. Reimann, J. B. Burkholder, C. Clerbaux, B. D. Hall, R. Hossaini, J. C. Laube, and S. A. Yvon-Lewis (2014), Ozone-depleting substances (ODSs) and other gases of interest to the Montreal Protocol, Chapter 1 in scientific assessment of ozone depletion: 2014, Global Ozone Research and Monitoring Project –Report No. 55, WMO, Geneva, Switzerland.

Chevallier, F., F.-M. Breon, and P. Rayner (2007), The contribution of the Orbiting Carbon Observatory to the estimation of CO_2 sources and sinks: Theoretical study in a variational data assimilation framework, *J. Geophys. Res.*, 112, D09307, doi:10.1029/2006JD007375.

Clodic, D., J. Baker, J. Chen, T. Hirata, R. Hwang, J. Kohler, C. Peotitjean, and A. Suwono (2005), *IPCC/TEAP Special Report. Safeguarding the Ozone Layer and the Global Climate System: Issues Related to Hydrofluorocarbons and Perfluorocarbons*, pp. 478, Cambridge Univ. Press, Cambridge, U. K., and New York.

Daniel, J., et al. (2011), A focus on information and options for policymakers, in *Scientific Assessment of Ozone Depletion: 2010, WMO Global Ozone Res. Monit. Proj. – Rep.*, vol. 52, chap. 5, pp. 5.1–5.56, WMO, Geneva, Switzerland.

Davis, S. C., S. W. Diegel, and R. G. Boundy (2012), *Transportation Energy Data Book*, 31st ed., Vehicle Technol. Program, Office of Energy Effic. and Renewable Energy, U.S. Dep. of Energy, Contract No. DE-AC05-00OR22725, Oak Ridge Natl. Lab., Oak Ridge, Tenn. [Available at cta.ornl.gov/data.]

EPA (2008), Direct HFC and PFC emissions from use of refrigeration and air conditioning equipment, Climate Leaders Greenhouse Gas Protocol, EPA430-K-03-004.

EPA (2014), Text of North American HFC phase-down amendment proposal. [Available at http://www.epa.gov/ozone/downloads/HFC_Amendment_2014_Text.pdf.]

Forster, P., et al. (2007), Changes in atmospheric constituents and in radiative forcing, in *Climate Change 2007: The Physical Science Basis. Contribution of Working Group I to the Fourth Assessment Report of the Intergovernmental Panel on Climate Change*, chap. 2, edited by S. Solomon et al., pp. 996, Cambridge Univ. Press, Cambridge, U. K., and New York.

Fortems-Cheiney, A., F. Chevallier, M. Saunois, I. Pison, P. Bousquet, C. Cressot, H. J. Wang, Y. Yokouchi, and F. Artuso (2013), HCFC-22 emissions at global and regional scales between 1995 and 2010: Trends and variability, *J. Geophys. Res. Atmos.*, 118, 7379–7388, doi:10.1002/jgrd.50544.

Gilbert, J., and C. Lemaréchal (1989), Some numerical experiments with variable-storage quasi-Newton algorithms, *Math. Program.*, 45, 407–435.

Harris, N. R. P., et al. (2014), Scenarios and information for policymakers, in *Scientific Assessment of Ozone Depletion: 2014, Global Ozone Res. and Monit. Proj. – Rep.*, vol. 55, chap. 5, WMO, Geneva, Switzerland.

Hauglustaine, D. A., F. Hourdin, L. Jourdain, M.-A. Filiberti, S. Walters, J.-F. Lamarque, and E. Holland (2004), Interactive chemistry in the Laboratoire de Météorologie Dynamique general circulation model: Description and background tropospheric chemistry evaluation, *J. Geophys. Res.*, *109*, D04314, doi:10.1029/2003JD003957.

Hourdin, F., I. Musat, S. Bony, P. Braconnot, and F. Codron (2006), The LMDZ4 general circulation model: Climate performance and sensitivity to parametrized physics with emphasis on tropical convection, *Clim. Dyn.*, *27*, 787–813, doi:10.1007/s00382-006-0158-0.

Hu, J., D. Wan, C. Li, J. Zhang, and X. Yi (2009), Forecasting of consumption and emission of HFC-134a used in automobile air conditioner sector in China, *Adv. Clim. Change Res.*, *5*, 1–6.

Hu, L., et al. (2015), US emissions of HFC-134a derived for 2008–2012 from an extensive flask-air sampling network, *J. Geophys. Res. Atmos.*, *120*, 801–825, doi:10.1002/2014JD022617.

Keller, C. A., et al. (2012), European emissions of halogenated greenhouses gases inferred from atmospheric measurements, *Environ. Sci. Technol.*, *46*, 217–225, doi:10.1021/es202453j.

Kim, J., et al. (2010), Regional atmospheric emissions determined from measurements at Jeju Island: Halogenated compounds from China, *Geophys. Res. Lett.*, *37*, L12801, doi:10.1029/2010GL043263.

Krol, M., and J. Lelieveld (2003), Can the variability in tropospheric OH be deduced from measurements of 1,1,1-trichloroethane (methyl chloroform)?, *J. Geophys. Res.*, *108*(D3), 4125, doi:10.1029/2002JD002423.

Kuijpers, L. (2011), Technical options committee refrigeration, A/C and heat pumps assessment report, ISBN 978-9966-20-002-0.

Lunt, M. F., et al. (2015), Reconciling reported and unreported HFC emissions with atmospheric observations, *Proc. Natl. Acad. Sci. U.S.A.*, *112*, 19. [Available at www.pnas.org/cgi/doi/10.1073/pnas.1420247112.]

Manning, A. J., and R. F. Weiss (2007), Quantifying regional GHG emissions from atmospheric measurements: HFC-134a at Trinidad Head, 50th Anniversary of the Global Carbon Dioxide Record Symposium and Celebration, Kona, Hawaii. [Available at http://www.esrl.noaa.gov/gmd/co2conference/pdfs/.]

Millet, D. B., et al. (2009), Halocarbon emissions from the United States and Mexico and their global warming potential, *Environ. Sci. Technol.*, *43*, 1055–1060.

Molina, M., D. Zaelke, K. M. Sarma, S. O. Andersen, V. Ramanathan, and D. Kaniaru (2009), Reducing abrupt climate change risk using the Montreal Protocol and other regulatory actions to complement cuts in CO_2 emissions, *Proc. Natl. Acad. Sci. U.S.A.*, *106*, 20,616–20,621, doi:10.1073/pnas.0902568106.

Montzka, S. A., R. C. Myers, J. H. Butler, J. W. Elkins, L. T. Lock, A. D. Clarke, and A. H. Goldstein (1996), Observations of HFC-134a in the remote troposphere, *Geophys. Res. Lett.*, *23*(2), 169–172, doi:10.1029/95GL03590.

Montzka, S. A., et al. (2011), Ozone-depleting substances (ODSs) and related chemicals, in *Scientific Assessment of Ozone Depletion: 2010*, *Global Ozone Res. and Monit. Proj.-Rep.*, vol. 52, chap. 1, pp. 516, WMO, Geneva, Switzerland.

Montzka, S. A., M. McFarland, S. O. Andersen, B. R. Miller, D. W. Fahey, B. D. Hall, L. Hu, C. Siso, and J. W. Elkins (2014), Recent trends in global emissions of hydrochlorofluorocarbons and hydrofluorocarbons: Reflecting on the 2007 adjustments to the Montreal Protocol, *J. Phys. Chem. A*, *119*, 4439–4449.

O'Doherty, S., et al. (2004), Rapid growth of HFC-134a, HCFC-141b, HCFC-142b and HCFC-22 from AGAGE observations at Cape Grim, Tasmania and Mace Head, Ireland, *J. Geophys. Res.*, *109*, D06310, doi:10.1029/2003JD004277.

Prinn, R. G., et al. (2000), A history of chemically and radiatively important gases in air deduced from ALE/GAGE/AGAGE, *J. Geophys. Res.*, *115*, 17,751–17,792, doi:10.1029/2000JD900141.

Prinn, R. G., et al. (2001), Evidence for substantial variations of atmospheric hydroxyl radicals in the past two decades, *Science*, *292*, 1882–1888.

Reimann, S., D. Schaub, K. Stemmler, D. Folini, M. Hill, P. Hofer, B. Buchmann, P. G. Simmonds, B. R. Greally, and S. O'Doherty (2004), Halogenated greenhouse gases at the Swiss high alpine site of Jungfraujoch (3580 m asl): Continuous measurements and their use for regional European source allocation, *J. Geophys. Res.*, *109*, D05307, doi:10.1029/2003JD003923.

Rigby, M., et al. (2014), Recent and future trends in synthetic greenhouse gas radiative forcing, *Geophys. Res. Lett.*, *41*, 2623–2630, doi:10.1002/2013GL059099.

Rugh, J., V. Hovland, and S. O. Andersen (2004), Significant fuel savings and emission reductions by improving vehicle air conditioning, Proceedings of the Mobile Air Conditioning Summit 2004, 15 April 2004, Washington, D. C., USA, Earth Technologies Forum, Arlington, Va.

Saba, S., R. Slim, L. Palandre, and D. Clodic (2009), Inventory of direct and indirect GHG emissions from stationary air conditioning and refrigeration sources, with special emphasis on retail food refrigeration and unitary air conditioning, Final Report for CARB.

Sander, S. P., et al. (2011), Chemical kinetics and photochemical data for use in atmospheric studies, Evaluation No. 17, JPL Publication 10–6, Jet Propulsion Lab., Pasadena. [Available at http://jpldataeval.jpl.nasa.gov.]

Schwarz, W., and J. Harnisch (2003), Establishing the leakage rates of mobile air conditioners; study carried out for DG Environment of the European Commission, Brussels. 17 April 2003. Contract number B4-3040/2002/337136/MAR/C1. [Available at http://www.europa.eu.int/comm/environment/climat/pdf/leakage_rates_final_report.pdf.]

Stohl, A., et al. (2009), An analytical inversion method for determining regional and global emissions of greenhouse gases: Sensitivity studies and application to halocarbons, *Atmos. Chem. Phys.*, *9*, 1597–1620.

Stohl, A., et al. (2010), Hydrochlorofluorocarbon and hydrofluorocarbon emissions in East Asia determined by inverse modeling, *Atmos. Chem. Phys.*, *10*, 3545–3560.

Su, S., X. Fang, L. Li, J. Wu, J. Zhang, W. Xu, and J. Hu (2015), HFC-134a emissions from mobile air conditioning in China from 1995 to 2030, *Atmos. Environ.*, *102*, 122–129.

U.S. Department of Transportation (2012), Federal Highway Administration, Highway Statistics 2010, Washington, D. C.

U.S. Energy Information Administration (2014), Monthly Energy Review Rep. DOE/EIA-0035(2014/01).

Velders, G. J. M., D. W. Fahey, J. S. Daniel, M. McFarland, and S. O. Andersen (2009), The large contribution of projected HFC emissions to future climate forcing, *Proc. Natl. Acad. Sci. U.S.A.*, *106*, 10,949–10,954.

Wallington, J., J. L. Sullivan, and M. D. Hurley (2008), Emissions of CO_2, CO, NO_x, HC, PM, HFC-134a, N_2O and CH_4 from the global light duty vehicle fleet, *Meteorol. Z.*, *17*(2), 109–116.

WARD (2010), Ward's motor vehicle data, pp. 287–290, Ward's Communications.

Wimberger, E. (2010), Emissions of HFC-134a in auto dismantling and recycling, Report prepared for the State of California Air Resources Board, Contract Number 06–334, revised on 16 July.

Xiang, B., et al. (2014), Global emissions of refrigerants HCFC-22 and HFC-134a: Unforeseen seasonal contributions, *Proc. Natl. Acad. Sci. U.S.A.*, *111*(49), 17,379–17,384.

Yao, B., M. K. Vollmer, L. X. Zhou, S. Henne, S. Reimann, P. C. Li, A. Wenger, and M. Hill (2012), In-situ measurements of atmospheric hydro-fluorocarbons (HFCs) and perfluorocarbons (PFCs) at the Shangdianzi regional background station, China, *Atmos. Chem. Phys.*, *12*, 10,181–10,193, doi:10.5194/acp-12-10181-2012.

Yokouchi, Y., T. Inagaki, K. Yazawa, T. Tamaru, T. Enomoto, and K. Izumi (2005), Estimates of ratios of anthropogenic halocarbon emissions from Japan based on aircraft monitoring over Sagami Bay, Japan, *J. Geophys. Res.*, *110*, D06301, doi:10.1029/2004JD005320.

Yokouchi, Y., S. Taguchi, T. Saito, Y. Tohjima, H. Tanimoto, and H. Mukai (2006), High frequency measurements of HFCs at a remote site in east Asia and their implications for Chinese emissions, *Geophys. Res. Lett.*, *33*, L21814, doi:10.1029/2006GL026403.